Available online at www.sciencedirect.com
SCIENCE DIRECT®
International Journal of Heat and Mass Transfer 48 (2005) 307–316
International Journal of HEAT and MASS TRANSFER
www.elsevier.com/locate/ijhmt

An integrated study of dropwise condensation heat transfer on self-assembled organic surfaces through Fourier transform infra-red spectroscopy and ellipsometry

Guoxin Pang, J. Doug Dale, Daniel Y. Kwok *

Nanoscale Technology and Engineering Laboratory, Department of Mechanical Engineering, University of Alberta, Edmonton, Alberta, Canada T6G 2G8

Received 29 March 2004; received in revised form 6 August 2004

Abstract

Self-assembled monolayers (SAMs) formed by adsorption of 1-octadecanethiol [$CH_3(CH_2)_{17}SH$] and 16-mercapto-hexadecanoic acid [$CO_2H(CH_2)_{15}SH$] onto gold-coated-copper substrates were applied to investigate the enhancement of dropwise condensation (DWC) heat transfer of steam at atmosphere pressure. A durability test was also conducted. Although hydrophobic SAMs increase the heat transfer coefficient by nearly an order of magnitude from that of filmwise condensation, it was found that DWC using octadecanethiol SAM as a promoter is a dynamic process in that the heat transfer coefficient decreases with time over 2 h. These results were reconfirmed by an integrated study using Fourier transform infra-red spectroscopy (FT-IR) and Spectroscopic Ellipsometry. We found that the monolayer of octadecanethiol becomes less crystalline with time, causing the film thickness and heat transfer coefficient to decrease. There was also some indications that, as SAMs were partly removed (leaving patches of the bare metal), contaminant from steam spontaneous adsorbed onto these high energy sites, resulting in a slightly higher heat transfer coefficient at a later stage of condensation.

1. Introduction

Condensation heat transfer is a vital process in the power generation industries. The two currently existing modes of condensation are filmwise and dropwise. Filmwise condensation (FWC) is currently used by industry while dropwise condensation (DWC) is an alternative that is under development. The latter offers attractive higher rates of heat transfer by preventing the build up of the insulating liquid layer found in filmwise condensation. For example, depending on the wettability (hydrophobicity) of surfaces, heat transfer coefficients of an order of magnitude larger than those associated with FWC can be achieved. The type of dominant condensation behavior relates directly to the surface energy of the condenser material or, more precisely, to contact angle phenomena. Typically, hydrophobic surface promotes DWC, whereas the hydrophilic one prefers FWC. It is a well known experimental fact that most of the heat

* Corresponding author. Tel.: +1 780 492 2791; fax: +1 780 492 2200.
E-mail address: daniel.y.kwok@ualberta.ca (D.Y. Kwok).

0017-9310/$ - see front matter © 2004 Elsevier Ltd. All rights reserved.
doi:10.1016/j.ijheatmasstransfer.2004.08.029

transfer in DWC occurs during the early stages of the formation and growth of a droplet. It must therefore be the aim of any pretreatment (a promoter) of the condenser surface to cause the condensate droplet to depart as early and as quickly from the condenser surface as possible. The departure of the drop is resisted by the adhesion of the droplet to the condenser surface, and this resistance is attributed to contact angle hysteresis.

Since it was first reported in 1930 by Schmidt et al. [1], DWC has been of interest to many investigators. The key point to the question has been, and is, to develop a reliable DWC promoter. Organic materials such as waxes, oils, and greases have been applied to achieve DWC of steam in the early 1960s; however, these promoters can be washed off rapidly and the condensation reverts to filmwise quickly. Noble metal coatings such as gold, silver, rhodium, palladium, and platinum have been found to produce excellent DWC [2]. For example, Woodruff and Westwater [3] studied DWC of steam on electroplated gold surfaces and found that a minimum thickness of 2000 Å of gold was required to obtain perfect dropwise condensation; otherwise film and dropwise condensation would coexist. A similar study for electroplated silver was conducted by O'Neil and Westwater [4]; they concluded that the life-time of using silver as a DWC promoter depends on the plating thickness, composition and the base metal preparation. It is noted that the dropwise characteristics of these noble metals as DWC promoters have been controversial. Bernett and Zisman [5] showed that pure water spontaneously wets noble metals which are free of organic or oxide contaminations. Theoretically, noble metal materials have higher surface energy than oils and should not exhibit DWC. However, DWC have been found using gold as the promoters, indicating that carbon (or organics) was probably the actual promoter. Woodruff and Westwater [6] have shown that the hydrophobicity of gold relates to the carbon to gold ratio on the surface. Thus, the heat transfer coefficient of DWC on noble metal surfaces depends on the coating methods and the operating environmental conditions.

Since the 1980s, thin-layer organic coatings with low surface energies have received more attention. For organic coatings, three factors restrict their applications to promote DWC. First, there must be a good, long-term adhesion between the coatings and metal substrates. However, it is well known that organic materials are more difficult to be sustained on metal substrates at elevated temperatures. Second, in general, the thicker the coating, the better its resistance to oxidation and erosion. However, the thickness of these organic coatings should not be larger than a few micrometers in order to minimize thermal conductivity; otherwise, enhancement of heat transfer coefficient will be compensated by the increase in thermal resistance of the coating itself [7]. Finally, if the coating materials gradually peel off from the substrates during DWC, it may contaminate the heat exchanger system and lead to other serious, unknown problems.

Nevertheless, development of ultra-thin and stable coatings for DWC are still of interest to researchers. Holden et al. [8] evaluated 14 polymer coatings for their abilities to promote and sustain DWC of steam at atmosphere pressure. Nine of the coatings have fluoropolymer as a major constituent; four has hydrocarbons and one with silicone. Six of these coatings were selected for applications to perform a heat transfer evaluation. Condensation results indicated that the steam-side heat transfer coefficient can be increased by a factor of five to eight through the use of polymer coatings. Ma et al. [9] coated ultra-thin polymers that were created by plasma polymerization and dynamic ion-beam mixed implantation (DIMI) method on vertical brass tubes for heat transfer experiment. It was concluded that, while the heat transfer enhancement was as high as 20 times, the promotion and the adhesion of the ultra-thin film with the substrate were strongly dependent on the process conditions of the two methods and require further study to optimize its performance. Subsequently, a lifetime test experiment was conducted [10]. These experimental results demonstrated that one surface had sustained DWC for about 1000 h. It was also found that polymer films prepared by DIMI had good adhesion with the metal substrate. In a different study, Ma et al. [11] investigated the influence of processing conditions for polymer films by means of the DIMI technique on dropwise condensation heat transfer. Their experimental results indicated that as heat flux was increased by 0.3–4.6 times, condensation heat transfer coefficient could increase 1.6–28.6 times when compared with those from FWC for the brass tubes treated with various conditions. Taniguchi and Mori [12] studied the effectiveness of composite copper/graphite fluoride platings to promote DWC of steam. It was confirmed that steam condensed dropwise on the platings. Despite their exceptionally strong "water repellency", they found no reduction in the critical departure size of condensate drops. A hypothetical explanation was made on the apparent inconsistency between the manner of water-to-plating contact in the air and that in a condensing steam. Zhao et al. [13] studied DWC of steam by three layers of barium stearates monomolecular film on the copper plate (30 mm in diameter) using Langmuir–Blodgett (LB) film balance. Dropwise condensation was formed on the surface in laboratory conditions. However, it is well-known that surface films formed by means of a LB balance are unstable due to its weak physical interactions with the original substrate [14].

Recently, Das et al. [15,16] applied an organic self-assembled monolayers (SAMs) coating to promote DWC of steam on horizontal tubes. The coating was

created with SAMs adsorbed onto gold, copper and copper-nickel alloy surfaces. The monolayers were formed by chemisorption of alkanethiols onto these metal surfaces. When compared to film condensation, their coatings increased the condensation heat transfer coefficient by factors of three to fourteen for different substrates under different conditions. The reason for using SAMs as DWC promoters is that SAMs formed by adsorption of hexadecylthiol [$CH_3(CH_2)_{15}SH$] on tube-metal surfaces creates a hydrophobic surface and hence should have DWC characteristics. The physico-chemical interactions between alkylthiol and metal are stronger than the physical interactions by means of the LB balance [14]. The condensing surfaces prepared by these SAMs were strong and lasted over a period of time. In addition, being only a monomolecular thick (10–15 Å), these coatings provide negligible heat transfer resistance, and the total amount of coating material involved is minuscule to pose any contamination problem. Therefore, it was concluded that self-assembled monolayers appears to offer a strong potential for long-term DWC promoters, although durability test was not explored.

We note that, although surface properties are crucial factors in DWC, there have been very little effort in the literature to relate the enhanced heat transfer coefficient directly with surface properties, chemistries, and property changes over time; documentation of the procedures for surface preparation and characterization are surprisingly limited. Here, we present an integrated study of dropwise condensation heat transfer on self-assembled monolayers of 1-octadecanethiol [$CH_3(CH_2)_{17}SH$] and 16-mercaptohexadecanoic acid [$CO_2H(CH_2)_{15}SH$] adsorbed onto gold-coated-copper substrates. The choice of these SAMs allows a systematic surface energetic variation in relation to the enhanced heat transfer coefficient. A durability test is also conducted by relating the heat transfer coefficient to changes in monolayer thickness and chemistry over time through a Spectroscopic Ellipsometry and a Fourier transform infra-red spectroscopy (FT-IR), respectively. Our integrated study indicates clearly the presence of a time-dependent kinetics for the organic surfaces during DWC process.

2. Materials and experimental methods

2.1. Self-assembled monolayers (SAMs)

Self-assembled monolayers form spontaneously by chemisorption and self-organization of functionalized, long-chain organic molecules onto the appropriate substrates [17]. The best characterized systems of SAMs are alkanethiolates [$X(CH_2)_nSH$] adsorbed onto gold surfaces. A schematic of a highly ordered monolayer of alkanethiolate formed on a gold-coated-copper surface is shown in Fig. 1. The process of self-assembly is believed to involve an oxidative addition of an S-H bond to the gold surface, followed by a reductive elimination of hydrogen:

$$X(CH_2)_nSH + Au^0 \rightarrow X(CH_2)_nS^-Au^+ \cdot Au_n^0 + 1/2\ H_2 \quad (1)$$

While debate still remains on the reaction mechanism, one conclusion has been reached unanimously; that is, the chemisorbed species on gold is a thiolate type [18]. Sulfur atoms bond to the gold surfaces and bring the alkyl chains into close contact; these contacts freeze out configurational entropy and lead to an ordered structure. It is noted that the sulfur/Au interaction is purely physiochemical and not by means of a covalent bonding [17], contrary to that claimed elsewhere [15]. For carbon chains of up to approximately 20 atoms, the degree of interaction for SAM increases with the density of molecules on the surface and the length of the alkyl backbones. It has been found that only alkanethiolates having chain length $n > 11$ form closely packed and essentially two-dimensional organic quasi-crystals supported on gold [17].

SAMs of alkanethiolates on gold exhibit many features that are most attractive about self-assembled systems [17]: ease of preparation, low density of defects, good stability under ambient laboratory conditions, and amenable to control interfacial properties (i.e. wettability). As an example, if the end functional group is methyl [–CH_3], the surface exhibits hydrophobic characteristics with water having contact angles between

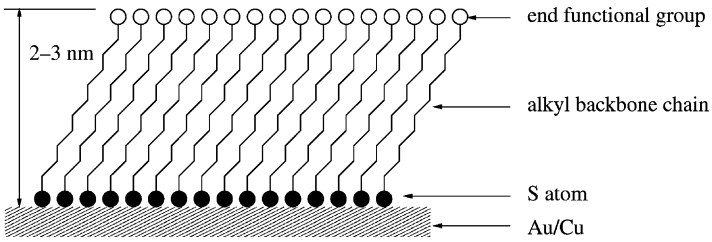

Fig. 1. Schematic of a highly ordered alkanethiolate monolayer adsorbed onto a gold-coated-copper (Au/Cu) surface.

110–118° [19,20]. If the end group is selected as carboxylic acid [–CO_2H], the surface would become hydrophilic having near zero contact angle for water. Furthermore, it has been experimental verified [19] that long-chain thiols form films that are thermally more stable than those from shorter chains. For $n < 14$, the contact angle of water on the surface composed of purely methyl groups are progressively lower; for longer chain thiols, the wetting properties are largely independent of chain length. Thus, we select 1-octadecanethiol ($n = 17$) here as the SAMs adsorbed onto gold-coated-copper substrate [$CH_3(CH_2)_{17}S$/Au/Cu] to be the DWC promoter. For comparison purpose, a higher-energy (more hydrophilic) SAM, 16-mercaptohexadecanoic acid adsorbed onto gold-coated-copper substrate [$CO_2H(CH_2)_{15}S$/Au/Cu] was employed for filmwise condensation.

2.2. Sample preparation

2.2.1. Condenser surface polishing

Condensation experiments were conducted on a vertical surface of rectangular blocks ($107.95 \times 31.75 \times 50$ mm) of pure copper (oxide free electrolytic copper). In order to reduce contact angle hysteresis due to roughness, the condensing surfaces were polished manually according to the following procedures for lapping, polishing and fine polishing:

1. Lapping: the copper block of interest was put onto a lapping machine (Lapmaster) using a 5 μm grit size alpha aluminum powder (E.T. Enterprises) suspended in mineral oil and varsol or portable heater fuel (Imperial Oil) until the entire surface appeared to be smooth. It was then rinsed thoroughly with ethanol and water in order to remove the oil and all coarse grains of the polishing compound.
2. Polishing: The above cleaned and smooth surface was polished by means of a high speed brass polishing wheel. The first step is to employ a Nylon polishing cloth (Buehler Ltd.) using a 6 μm grit size diamond polishing compound (Hyprez) and a Diamet fluid (E.T. Enterprises). This was followed by cleaning the block with ethanol for removal of the oil used. The next step is to employ a pellon polishing cloth (E.T. Enterprises). The polishing grade is a 1 μm Diamet diamond suspension (E.T. Enterprises). This process removes large scratches left from lapping and results in a highly reflective surface. Before moving onto the next procedure, the copper block was cleaned in an ultrasonic cleaner filled with deionized ultra filtered (DIUF) water (Fisher Scientific) for 15 min.
3. Fine Polishing: Fine polishing was conducted on a micro-polishing cloth (E.T. Enterprises) using a relatively slower rotating brass polishing wheel. A 0.3 μm and subsequently a 0.05 μm grit size of aluminum oxide Powder (Beta Diamond Products Inc.) suspended in DIUF water were used as the polishing grade. Between each fine polishing steps, the block was rinsed with DIUF water, methanol and acetone (Fisher Scientific) to remove possible traces of organic materials.

The final polishing produced surfaces virtually similar to a mirror finish. The copper block was then kept in a chemical-resistant vacuum desiccator (Fisher Scientific) to prevent contamination from surroundings.

2.2.2. Thermal evaporation

Although self-assembled monolayers spontaneous adsorbed onto pure copper surface, experience has shown that SAMs prepared on such surface is of poor quality and depends very much on the history of sample preparation. This is due to the fact that copper oxidizes quickly upon exposure to air and hence the structure of SAMs on copper is extremely sensitive to its oxidation history, resulting in poor reproducibility of the experiment. For this reason, a titanium and subsequently a gold layer were coated onto the condensing copper surface by a vacuum vapor deposition technique. Here, the thin layer of titanium is called a "glue layer", which serves as an adhesion promoter between the substrate (copper) and gold. The thickness of titanium and gold are 15 and 100 nm, respectively; hence, their heat transfer resistances are negligible comparing with that of the copper block (50 mm thick). Preparation of these coatings is described by the procedures below: Our polished copper blocks were placed in a diffusive-pumped vacuum chamber where ~150 Å of titanium (99.9995%, Kurt J. Lesker Co.) and ~1000 Å of gold (99.999%, Kurt J. Lesker Co.) were sequentially evaporated from tungsten holders onto the copper blocks at a maximum evaporation rate of $\leqslant 2$ Å/s and a pressure of $\leqslant 2 \times 10^{-6}$ Torr. Deposition rates and mass thickness were monitored using an Infinicon XTM/2 quartz crystal monitor. After evaporation, the chamber was then slowly backfilled with air and the coated copper blocks were removed immediately for monolayer assembly, similar to those prepared elsewhere [20].

2.2.3. Deposition of SAMs

Immediately after taken out from the chamber, the copper blocks were thoroughly rinsed with ethanol and dried with a nitrogen jet. The blocks were then made in "contact" with either a 5 mM 1-octadecanethiol (Aldrich) or 16-mercaptohexadecanoic acid (Aldrich) ethanolic (100%, Univ. of Alberta) solutions for 1 h. Typically, SAMs are formed by immersing the entire surface into the alkanethiol solution [20]. However, we found that this procedure does not produce good struc-

ture of SAMs, as indicated by Fourier-Transform Infra-red (FT-IR) results. This poor structure can lead to erroneous interpretation of condensation data. Although the reason for this cause is unclear, we found that placing a copper block upside down and allowing only the condenser surface to be in contact with the alkanethiolate solution produces good quality of SAMs which are comparable with those in the literature [19,20]. After SAMs formation, the samples were rinsed sequentially with ethanol and DIUF water, and blown dry with nitrogen before use.

2.3. Experimental apparatus

2.3.1. Fourier transform infra-red spectroscopy (FT-IR)

The quality of SAMs before and after the condensation experiments was detected using a Fourier transform infra-red spectroscopy (Nexus 670, Thermo Nicolet). A Pike VeeMax accessory with a grazing angle of 75° from the surface normal and a polarizer set to 90° so as to minimize light scattering from the surface were used. The reflected infra-red signal was detected using a liquid N_2 cooled MCT-A detector. Spectra resolution was set to 0.964 cm^{-1} for data collection in reference to the bare Au substrate. To increase the signal-to-noise ratio, 512 scans of the spectra were collected for each sample.

2.3.2. Spectroscopic ellipsometry

The variation of SAMs thickness during the condensation experiments were determined using a Variable Angle Spectroscopic Ellipsometry (SOPRA GESP 5). The ellipsometry measurements were taken by linear polarizing a beam of light from a 75 W Xe-arc lamp using a polarizer rotating at 8 Hz and directing onto the surface at a 75° angle from the surface normal. The data for tan Ψ and cos Δ were collected over a visible light range (300–850 nm) using a rotating analyzer in a current tracking mode [20]. The data sets of tan Ψ and cos Δ for the SAMs/Au/Cu surfaces were compared against with those on a reference bare Au/Cu substrate. This difference in tan Ψ and cos Δ allows calculation of the corrected monolayer thickness.

2.3.3. Experimental set-up

Fig. 2 shows schematically the experimental set-up for the measurements of condensation heat transfer coefficient. Steam is generated by a hot shot electric steam boiler (Automatic Steam Products Corporation, NY), which is filled automatically with domestic water supply from the building. As shown in Fig. 2, steam flows through a stainless steel tubing, regulator and condenser control valve before entering the condensing chamber and condensing on the copper surface. A steam trap was used to separate the condensed liquid steam in the flowing process. All condensate and excess steam which do not condensed in the test section will pass through the secondary condenser and are measured in a standard glass tube flow meter (Omega). The secondary condenser was designed to condense all remaining steam, so that the mass flow rate of the condensate water will be the same as that of the steam passing through the condensing chamber. Combining this with the cross-sectional area and condensation pressure measured from a pressure gauge in the condensing chamber, a steam

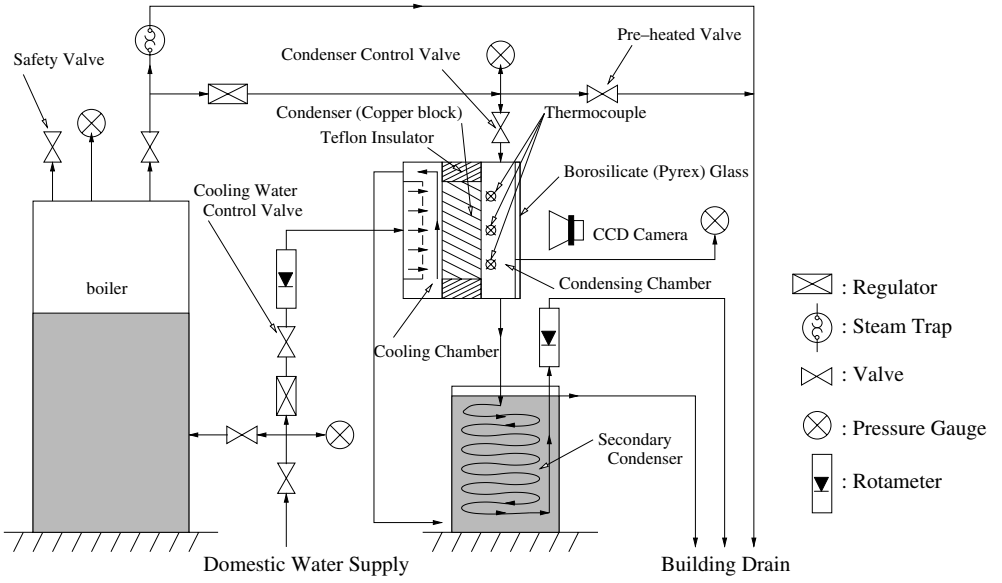

Fig. 2. Schematic of an experimental set-up for the measurements of condensation heat transfer coefficient.

velocity passing through the condensing surface can be calculated. The height of the flow meter was calibrated before all condensation experiments as it would alter the pressure of the condensing chamber. By adjusting the condenser control valve and height of the flow meter, an expected condensation pressure and steam velocity can be obtained. In this study, all experiments were conducted at atmosphere pressure. A higher, but constant, steam velocity was used in order to eliminate the effect of non-condensible gas [21].

Domestic water from the building was also used as the coolant. To ensure a steady flow for the cooling system, the exit pressure of the coolant water passing through a regulator was maintained constant. The flow rate was adjusted through the cooling water control valve to obtain the expected heat flux by monitoring the glass tube full-view flow meter (Brooks Instrument). After flowing through the cooling chamber and the secondary condenser subsequently, the coolant water is drained with the condensate of the system. Details of these experimental set-up can be found elsewhere [22].

3. Measurement principle

Fig. 3 shows a schematic of the measurement system for the copper block condenser. Two assumptions were made in the calculations:

1. One-dimensional steady-state conduction heat transfer along the "X" direction was assumed. The copper block was insulated by a thick Teflon (PTFE) block and two Teflon rings from the surroundings so that heat loss in other directions could be neglected.
2. The thermal conductivity of the copper block was assumed constant in each region of δ_0, δ_1, δ_2, and δ_3 which depend on the temperatures T_1, T_2, T_3, and T_4, respectively. The relationship between thermal conductivity of copper and temperature can be obtained by polynomial regression.

According to these assumptions, a heat transfer coefficient can be determined from the following relationships:

$$h = \frac{q''}{T_{\text{steam}} - T_{\text{surface}}} \tag{2}$$

and

$$q'' = -k \cdot \frac{\mathrm{d}T}{\mathrm{d}x} \tag{3}$$

where the heat flux q'' was obtained by averaging the heat flux through the copper block

$$q'' = \frac{1}{3} \cdot \left(K_2 \cdot \frac{T_1 - T_2}{\delta_1} + K_3 \cdot \frac{T_2 - T_3}{\delta_2} + K_4 \cdot \frac{T_3 - T_4}{\delta_3} \right) \tag{4}$$

A mean temperature of the condensing surface T_{surface} was calculated by extrapolating the temperature profile from the copper block

$$T_{\text{surface}} = T_1 + \frac{q''}{K_1} \cdot \delta_0 \tag{5}$$

Thus, only the following five temperatures (T_1, T_2, T_3, T_4, and T_{steam}) and four distances (δ_0, δ_1, δ_2, and δ_3) are experimental quantities.

The temperatures T_1, T_2, T_3, and T_4 were determined by inserting four Type T (copper vs. copper–nickel)

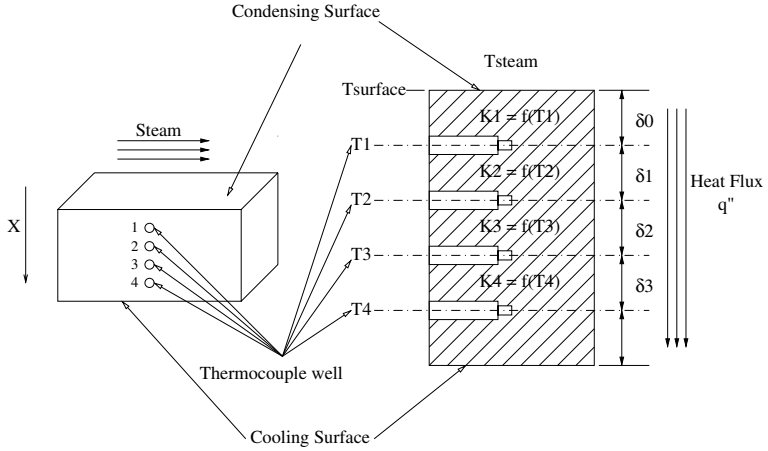

Fig. 3. Schematic of the measurement system of the copper block condenser.

miniature quick disconnect small diameter thermocouple probes (Wika Instruments Ltd., Edmonton) into the thermocouple wells of the copper block. The spacings between these thermocouple probes (0.02 in. diameter) and the tip of the thermocouple well (0.025 in. diameter) were filled with a thermal compound (Wakefield Engineering Inc.) to ensure perfect contact between the thermocouple and copper block. T_{steam} was measured by three Type T thermocouple wires (Minco Products Inc.) mounted into the condensing chamber. This value of T_{steam} was compared with the saturation temperature corresponding to the condensing steam pressure obtained by the pressure gauge connected to the condensing chamber (see Fig. 2).

All thermocouples were calibrated in a variable temperature oil bath (Model 910AC, Rosemount Engineering Co.) against a thermometry system (2189A, Fluke), which consists of a 2180A digital thermometer (with microcomputer Type 2) and a Y2039 resistance temperature probe. The calibration coefficient for each thermocouple was obtained by a second order polynomial regression. The output and calibration coefficients of all thermocouples were input into a data acquisition system, which includes a PCI-DAS-TC board (Measurement Computing Corp.) and a computer with a data acquisition software (LabView). By a Root-Sum-Square criterion [23], the maximum error of these thermocouples is reduced from 1.0 °C to 0.26 °C after calibration with a relative maximum error of less than 1%. After the thermocouple well were drilled, the exact distances (δ_0, δ_1, δ_2, and δ_3) were measured by a Leitz universal toolmaker microscope (Model UMW, Leitz Wetzlar). Through the Root-Sum-Square criterion [23], the maximum error was calculated to be less than 0.09 mm. Comparing with the height of copper block (50 mm), this relative maximum error is indeed less than 1%, which is more than sufficient for the calculation of heat transfer coefficients in this study.

4. Results and discussion

4.1. Improvement of heat transfer coefficient

Condensation experiments were first conducted on the hydrophilic 16-mercaptohexadecanoic acid SAMs as we expect film condensation would occur. The experimental heat transfer coefficients h with time are displayed in Fig. 4 for a heat flux q'' of 300 kW/m^2 and a subcooling temperature ΔT of 32 °C. Those heat transfer coefficients calculated by the Nusselt theory for film condensation on a vertical plate [4,24] are also given in the same figure. It can be seen that the experimental h for the 16-mercaptohexadecanoic acid is stable for more than 2 h and agree with those predicted from the Nusselt

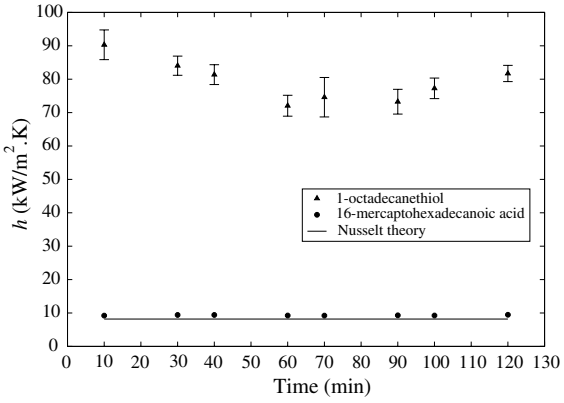

Fig. 4. Condensation heat transfer coefficient of SAMs on evaporated Au/Ti/Cu substrates as a function of time during steam condensation at atmosphere pressure. Steam velocity passing through the condensing surface is around 6 m/s.

theory, suggesting that our procedures and experimental setup for the determination of heat transfer coefficient h is valid.

A series of DWC experiments were carried out by using octadecanethiol SAMs as the promoter because of its hydrophobicity. The steam velocity and condensation pressure were maintained the same as that of the FWC experiments. The experimental results over time for an average of 5 independent tests are also given in Fig. 4 with a heat flux q'' of 320 kW/m^2. It should be point out that the error bars in Fig. 4 are the 95% confidence limits and the overall confidence intervals are within ±5%. Fig. 5 illustrates a picture of DWC of steam on the 1-octadecanethiol SAMs. As can be seen in Fig. 4, the DWC heat transfer coefficient is in the order of 70–90 kW/m^2 K, depending on the time of experiments. This represents nearly an order of magnitude improvement over FWC and is similar to those reported by

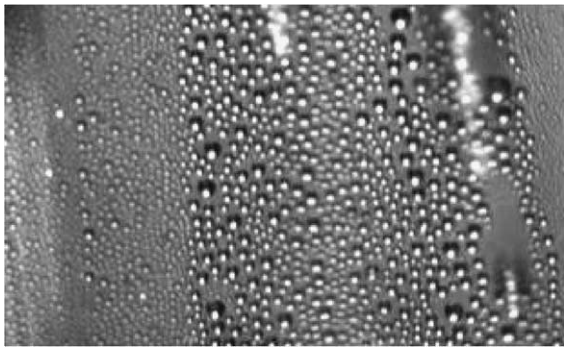

Fig. 5. Dropwise condensation of steam on self-assembled monolayers (SAMs) derived from 1-octadecanethiol [$HS(CH_2)_{17}CH_3$] onto gold-coated-copper substrates.

Das et al. [15,16]. While Das et al. reported a constant h value for the $HS(CH_2)_{15}CH_3$ for each heat flux, our results reveal that h is indeed time dependent; the heat transfer coefficient h starts at 90 kW/m^2 after 10 min of experiment and decreases to 70 kW/m^2 after about 1 h; eventually, it bounds back to 80 kW/m^2 after about 2 h. As SAMs are more stable the longer its chain length (up to about 22 carbons), we expect the $HS(CH_2)_{15}CH_3$ SAMs used in [15,16] to yield even a larger variation of h with time. Thus, we were interested in the apparent difference of our results and those reported in [15,16]. If the dynamic process of DWC on the $HS(CH_2)_{17}CH_3$ octadecanethiol is real, we speculate that its surface properties would have changed over time. To elucidate this, we employed ex situ FT-IR and ellipsometry to monitor the changes in surface chemistry and film thickness, respectively.

4.2. Characterizations of SAMs

To relate the changed DWC heat transfer coefficient with the actual surface chemistry, we employed ex situ Fourier transform infra-red spectroscopy (FT-IR) and Ellipsometry to characterize the SAMs during the condensation process. Our octadecanethiol monolayers were first characterized by reflectance Fourier transform infra-red spectroscopy (FT-IR) and ellipsometry in terms of spectra and thickness, respectively, before the condensation experiment, i.e. at $t = 0$. The copper block was then placed into the condenser for half an hour of condensation experiment before it was taken out for another surface characterization. These procedures were repeated several times in every 30 min until an elapse time of 2 h have reached. During surface characterization experiments, the copper block was labeled to ensure that the measured spectra and thickness are on the center of the condensing surface at each intervals. Fig. 6 displays the reflectance infra-red spectra for SAMs derived from octadecanethiol on gold-coated-copper substrates subjected to the condensation process at various duration for $q'' = 320$ kW/m^2. Figs. 7 and 8 show, respectively, the normalized thickness and heat transfer coefficient as a function of condensation duration, each for $q'' = 320$ and 360 kW/m^2. In Fig. 8, the error bars are 95% confidence limits and the overall confidence intervals are within ±5% for $q'' = 320$ kW/m^2 and ±7% for $q'' = 360$ kW/m^2.

In Fig. 6 for $t = 0$, the asymmetric methylene peaks $\nu_a(CH_2)$ appeared at ~2918 cm^{-1}, indicating a primarily trans-zigzag extended hydrocarbon chain with few gauche conformers. The spectra demonstrate that SAMs of octadecanethiol adsorbed onto Au are highly crystalline. This is independently confirmed by the ellipsometry results that our initial thickness was 22.3 Å at $t = 0$, in excellent agreement with the theoretical thickness of 22 Å [25] and those reported in the literature [20,26] for a closely packed octadecanethiol adsorbed onto gold. For $t > 0$, however, it can be seen in Fig. 6 that

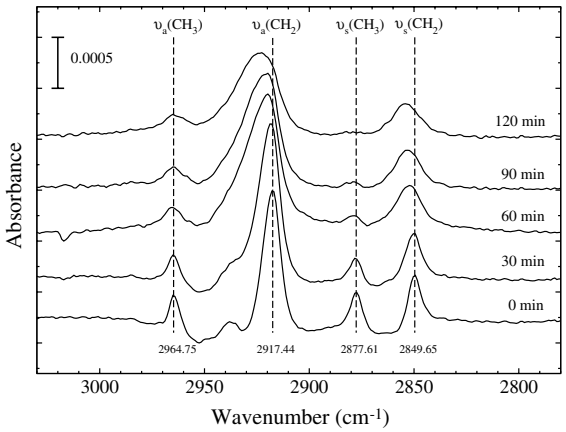

Fig. 6. Reflectance FT-IR spectra for SAMs derived from 1-octadecanethiol on gold-coated-copper substrates subjected to condensation in various duration ($q'' = 320$ kW/m^2). The dashed lines represent the positions of the original modes for a trans-extended monolayer. The spectra have been offset for clarity.

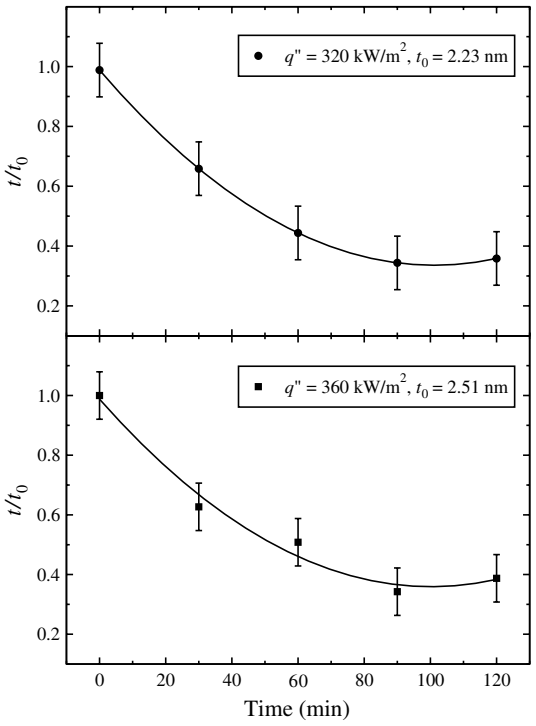

Fig. 7. Normalized thickness of SAMs derived from 1-octadecanethiol on gold-coated-copper substrates as the function of condensation duration for two heat fluxes ($q'' = 320$ and 360 kW/m^2). t_0 is the initial film thickness reference. Error bars are ±2 Å in reference to t_0 and represent typical measurement errors for the ellipsometry used during this study.

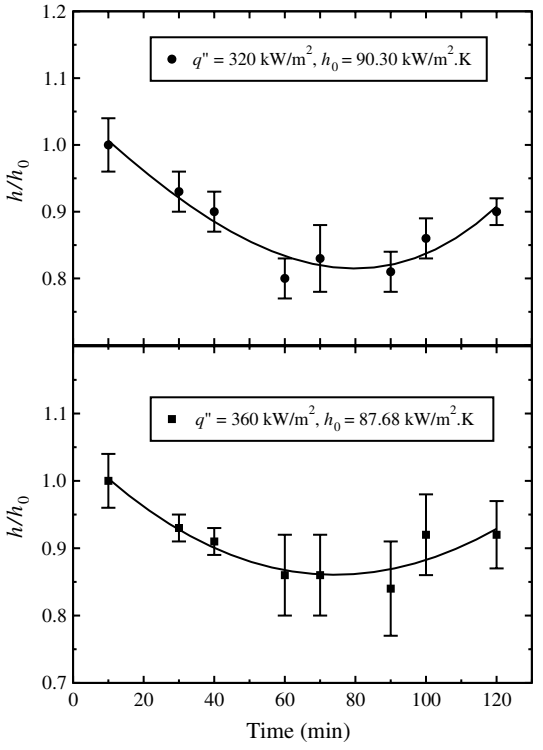

Fig. 8. Normalized heat transfer coefficient as a function of condensation duration for two heat fluxes ($q'' = 320$ and $360\,kW/m^2$). Error bars are 95% confidence limits.

nearly all spectra intensities decrease with the time of condensation, suggesting lost of monolayer with time. For trans-zigzig and highly-ordered conformations, the methylene asymmetric $v_a(CH_2)$ and symmetric $v_s(CH_2)$ modes should be below $2918\,cm^{-1}$ and $2850\,cm^{-1}$, respectively [20,26]. Deviation of the methylene peak positions from these values for $t > 0$ reflects that these monolayers have become less crystalline [27–29]. During condensation process, the intensity of the asymmetric methylene $v_a(CH_2)$ stretching mode increases slightly after 30 min and began to decrease continuously with time; while all intensities for $v_s(CH_2)$, $v_a(CH_3)$ and and $v_a(CH_3)$ decrease with time. We also note that the spectra exhibit peak broadening for all C-H stretching modes with time. These results indicate that the octadecanethiol SAMs are still crystalline at $t = 30$ min; while some monolayers have already been peeled off after 30 min. Thus, the tilt angle of the alkyl chain increases from the surface normal, exposing more methylene groups to the surface and resulting in the initial increase in $v_a(CH_2)$. After 90 min, the intensity of $v_s(CH_3)$ is nearly zero, suggesting that the monolayers are loosely packed and the infra-red hardly sees any methyl groups as they are blocked by the flexible methylene backbone. This interpretation is confirmed by the independent ellipsometry results in Fig. 7 that the normalized film thickness decreases with time and reaches a plateau after $t = 90$ min for both heat fluxes. Here, the condenser surface appears to have patches of the bare metals without the monolayers and should result in a mixture of dropwise and filmwise condensation. The lost in SAMs indicated from the above FT-IR and ellipsometry results are in good agreement with the general behavior of the experimental heat transfer coefficient h with time as shown in Fig. 8. It can be seen that as SAMs become less crystalline (decrease in thickness), the heat transfer coefficient decreases gradually during the first 90 min condensation process.

A very interesting phenomenon, however, occurs in Fig. 8. As SAMs are being partially removed exposing patches of bare gold after $t = 90$ min, we would expect a mixture of filmwise and dropwise condensation to coexist because gold is a high energy surface and steam condensate should spontaneously wet on these exposed bare gold patches [30]. If this is the case, it should reduce the total effective heat transfer coefficient. This expectation is not met in Fig. 8 as h, however, increases with time after $t = 90$ min. The reason for this phenomenon is not clear and requires further study. Presumably, when SAMs are partially removed exposing patches of the bare metal, contamination from steam would quickly adsorb on such high energy sites as gold has the ability to attract organic contaminations which are the "true" DWC promoters [2–6]. This causes localized DWC and results in a slightly higher effective heat transfer coefficient. This speculation is partly confirmed from the results in Fig. 7 that the film thickness increases slightly after $t = 90$ min. The conclusions obtained here would not have been possible without the use of infrared spectroscopy and ellipsometry. We conclude that surface properties are important factors in dropwise condensation. Understanding this process through surface modifications of organic monolayers requires careful experimentation and analytical tools.

5. Conclusions

We have performed an integrated study of dropwise condensation using self-assembled monolayers (SAMs) adsorbed onto gold-coated-copper substrates by means of Fourier transform infra-red spectroscopy and Spectroscopic Ellipsometry. 1-octadecanethiol and 16-mercaptohexadecanoic acid were employed as the coatings for dropwise and filmwise condensation, respectively, on vertical surface. We found that filmwise condensation results for the latter are in good agreement with those from the Nusselt theory. When the former was employed as a promoter, heat transfer coefficient increased by nearly an order of magnitude due to dropwise condensation. It was also found that dropwise condensation on

the octadecanethiol SAMs is a dynamic process, resulting in time-dependent of heat transfer coefficient. These results were reconfirmed, for the first time, through Fourier transform infra-red spectroscopy (FT-IR) and Spectroscopic Ellipsometry studies. In general, decrease in SAMs' crystallinity and thickness cause the heat transfer coefficient to decrease at a later stage. Partial removal of SAMs exposes the bare metal to the steam. Spontaneous adsorption of contamination onto these high energy patches appears to cause the heat transfer coefficient to increase. We also found that the thermal stability of self-assembled monolayers derived from adsorption of 16-mercaptohexadecanoic acid and 1-octadecanethiol onto gold substrates when exposed to steam are different.

Acknowledgments

This research was supported financially by the Natural Sciences and Engineering Research Council (NSERC) of Canada, Canada Research Chair (CRC) Program, and Canada Foundation for Innovation (CFI) to DYK. GP acknowledges support from the Province of Alberta through an Alberta Ingenuity studentship (No. 200200093).

References

[1] E. Schmidt, W. Schurig, W. Sellschopp, Tech. Mech. Thermodynam. 1 (1930) 53.
[2] R. Erb, E. Thelen, Tech. Rep., Washington, DC, (1965).
[3] D.W. Woodruff, J.W. Westwater, Int. J. Heat Mass Transfer 22 (1979) 629.
[4] G.A. O'Neill, J.W. Westwater, Int. J. Heat Mass Transfer 27 (1984) 1539.
[5] M. Bernett, W. Zisman, J. Phys. Chem. 74 (1970) 2309.
[6] D.W. Woodruff, J.W. Westwater, ASME J. Heat Transfer 103 (1981) 685.
[7] P.J. Marto, D.J. Looney, J.W. Rose, A.S. Wanniarachchi, Int. J. Heat Mass Transfer 29 (1986) 1109.
[8] K.M. Holden, A.S. Wanniarachchi, P.J. Marto, D.H. Boone, J.W. Rose, ASME J. Heat Transfer 109 (1987) 768.
[9] X. Ma, D. Xu, J. Lin, Heat Transfer 3 (1994) 359.
[10] X. Ma, B. Wang, D. Xu, J. Lin, Heat Transfer Asian Res. 28 (1999) 551.
[11] X. Ma, J. Chen, D. Xue, J. Lin, C. Ren, Z. Long, Int. J. Heat Mass Transfer 45 (2002) 3405.
[12] A. Taniguchi, Y.H. Mori, Int. Comm. Heat Mass Transfer 21 (1994) 619.
[13] Q. Zhao, D. Zhang, J. Lin, G. Wang, Chem. Eng. Proc. 35 (1996) 473.
[14] D.Y. Kwok and A.W. Neumann, Contact Angle Techniques and Measurements in Surface Characterization Methods: Principles, Techniques, Applications, Surfactant Science Series87 (Marcel Dekker, 1999), first ed.
[15] A.K. Das, H.P. Kilty, P.J. Marto, G.B. Andeen, A. Kumar, ASME J. Heat Transfer 122 (2000) 278.
[16] A.K. Das, H.P. Kilty, P.J. Marto, A. Kumar, G.B. Andeen, Enhanced Heat Transfer 7 (2000) 109.
[17] Y. Xia, G. Whitesides, Angew. Chem. Int. Ed. 37 (1998) 550.
[18] Y. Li, J. Huang, J.R.T. Mclver, J.C. Hemminger, J. Am. Chem. Soc. 114 (1992) 2428.
[19] C.D. Bain, E.B. Troughton, Y. Tao, J. Evall, G.M. Whiteside, R.G. Nuzzo, J. Am. Chem. Soc. 111 (1989) 321.
[20] J. Yang, J. Han, K. Isaacson, D.Y. Kwok, Langmuir 19 (2003) 9231.
[21] D.W. Tanner, D. Pope, C.J. Potter, D. West, Int. J. Heat Mass Transfer 8 (1965) 419.
[22] G. Pang, Master's thesis, University of Alberta (2004).
[23] F.S. Tse, I.E. Morse, Measurement and Instrumentation in Engineering: Principles and Basic LaM. Dekker Inc., M. Dekker, Inc., New York, 1989.
[24] F.P. Incropera, D.P. DeWitt, Introduction to Heat Transfer, third ed., John Wiley & Sons, 1996.
[25] H. Ron, S. Matlis, I. Rubinstein, Langmuir 14 (1998) 1116.
[26] P.E. Laibinis, G.M. Whitesides, D.L. Allara, Y.T. Tao, A.N. Parikh, R.G. Nuzzo, J. Am. Chem. Soc. 113 (1991) 7152.
[27] G.K. Jennings, P.E. Laibinis, J. Am. Chem. Soc. 119 (1997) 5208.
[28] R.G. Nuzzo, L.H. Dubois, D.L. Allara, J. Am. Chem. Soc. 112 (1990) 558.
[29] G.K. Jennings, J.C. Munro, T. Yong, P.E. Laibinis, Langmuir 14 (1998) 6130.
[30] D.G. Wilkins, L.A. Bromley, S.M. Read, AICHE Journal 19 (1973) 119.